

Article

Evaluation and Validation of Photovoltaic Potential Based on Time and Pathway of Solar-Powered Electric Vehicle

Chanwook Park ¹, Haneul Park ¹, Hwanhee Jeon ¹, Kyoik Choi ² and Jangwon Suh ^{2,*} ¹ Division Energy Engineering, Kangwon National University, Samcheok 25913, Republic of Korea² Department of Energy and Mineral Resources Engineering, Kangwon National University, Samcheok 25913, Republic of Korea

* Correspondence: jangwonsuh@kangwon.ac.kr; Tel.: +82-33-570-6313

Abstract: This study evaluates and validates the power output potential of using the travel time and driving route of a photovoltaic (PV)-powered electric vehicle (EV). A scenario was constructed wherein a car with modules attached to four sides (roof, rear window, left door, and right door) drove on seventeen road sections with various inclinations and azimuths. The shadow effect of the surrounding terrain and buildings was considered to assess the PV potential. Consequently, it was possible to analyze the differences in the potential of the four modules in the same or two sections with different topographies. It was determined that the car could produce 0.0158 kWh for a single drive (approximately 10 min) and 221 kWh for one year (considering six hours a day). The potential of the roof module was the highest, followed by those of the rear and two doors. The potentials of the modules attached to the rear window and side doors were calculated to be approximately 42% and 27%, respectively, of the roof module potential. Furthermore, the possibility of enhancing the potential of future PV-powered EVs was discussed. The results obtained in this study can be used to develop power-output algorithms and navigation solutions for PV-powered EVs.

Keywords: photovoltaic (PV); electric vehicle (EV); PV-powered EV; solar car; potential



Citation: Park, C.; Park, H.; Jeon, H.; Choi, K.; Suh, J. Evaluation and Validation of Photovoltaic Potential Based on Time and Pathway of Solar-Powered Electric Vehicle. *Appl. Sci.* **2023**, *13*, 1025. <https://doi.org/10.3390/app13021025>

Academic Editors: Diogo Canavarro and Manuel Collares-Pereira

Received: 30 December 2022

Revised: 10 January 2023

Accepted: 10 January 2023

Published: 12 January 2023



Copyright: © 2023 by the authors. Licensee MDPI, Basel, Switzerland. This article is an open access article distributed under the terms and conditions of the Creative Commons Attribution (CC BY) license (<https://creativecommons.org/licenses/by/4.0/>).

1. Introduction

To transition into a carbon-neutral society in the era of global climate crisis, countries worldwide are increasing the proportion of clean energy that can replace fossil fuels [1]. Particularly, the automobile industry, which uses fossil fuels as its main fuel source, is considered a cause of the climate change. To reduce carbon dioxide emissions, governments worldwide have banned the sale of internal combustion locomotive vehicles and prepared to switch to electric vehicles (EVs) or hydrogen vehicles (HVs) [2]. The European Union (EU) aims to attain carbon neutrality by presenting the goal of reducing carbon emissions from new cars by 55% by 2030 and 100% by 2035, compared to 2021 [3]. Accordingly, the paradigm of automobile market is shifting from internal combustion engine vehicles to EVs or HVs. Global automobile companies, including Tesla, Volkswagen, Volvo, and Hyundai Motor Company, have announced various EVs models and expanded their production [4]. However, several limitations prevail, including short mileage, battery lifespan (sustainability), shortage of electric charging infrastructure, and the method of charging or replacing batteries at electric charging stations [5].

Photovoltaic (PV)-powered EV (also called solar cars) have attracted attention as measures to alleviate the aforementioned problems in the operation and management of EVs. PV-powered EV have modules attached to the exterior (e.g., the roof of the vehicle) or are integrated into exterior materials (vehicle-integrated PV, VIPV) for self-charging using a solar energy source while driving or parking [6]. Therefore, they are eco-friendly because they do not emit carbon dioxide, require less charging compared to the general EVs, and minimize fuel costs [7]. Numerous commercialized PV-powered EV models have

been released, including Sion (Sono Motors), Lightyear One (Lightyear), Solar O, L, R, and A (Hanegy), Luna (Aptera Motors), Vision EQXX (Mercedes-Benz), Solar Prius (Toyota), Sonata (Hyundai Motor Group), and Revero (Karma Automotive) [4]. The global market size of PV-powered EV is expected to exceed 4.5 billion US dollar (USD) per year in 2030 [8]. However, efforts are required to overcome limitations, such as low efficiency of solar cells, small exterior surface area of vehicles, and variability of power output based on time and location [9].

Many recent studies have sought to develop technologies that ensure the commerciality and applicability of PV-powered EV. Yamaguchi et al. [7,10] assessed the effects of the development of high-efficiency solar cells on increasing the drivable distance and presented the anticipated effects of reducing carbon dioxide, EV charging cost, and battery capacity by adopting PV-powered EV. To develop high-efficiency or low-cost solar cells and modules applicable to PV-powered EV, Japanese researchers have reviewed the applicability of various types of solar cells and presented the expected cost reductions or effects [11,12]. PV-powered EV charging stations have been widely investigated, including the analysis of their feasibility, performance, suitability, and technical and economic impacts [13–18]. Several studies have been conducted on optimal parking lots, and researchers have predicted the amount of charge during the parking time of PV-powered EVs or suggested an optimal parking location based on geospatial analysis, considering solar irradiation and shadow effects at the site [19–21]. Recently, a method has been proposed for modeling shaded areas over time, creating a shading matrix representing the hourly shaded area ratio for a point on the road or parking space [22], and comparing the accuracy of two approaches, such as modeling and field measurement [23]. Additionally, several studies have analyzed the optimal driving pathways or routes of PV-powered EV [24–28].

Recently, the estimation of the potential of solar mobility has been demonstrated. Seo [29] estimated the PV potential of a vehicle with a module attached to the roof while moving on an expressway section 120 km long, considering the changes in solar radiation, shaded area based on time and location, and tunnel sections. Oh et al. [30] developed a power output prediction model for a solar bus with a solar roof attached and conducted a validation experiment to compare the predicted and observed values. Kim et al. [31] assumed that the module was attached to the roof of a solar train and developed an algorithm for predicting the PV potential considering solar irradiation and shadow effects that vary with time and location during operation. However, these studies have limitations in that they evaluated the PV potential by assuming that the module was attached only to the roof of the mobile device (Table 1). Furthermore, no study has evaluated the potential by considering the following four sides: Bonnet, rear window, left door, right door, and roof of the vehicle. First-generation PV-powered EV have only one module on the roof; however, next-generation models are expected to adopt translucent solar cells on glass and lightweight solar cells on the bonnet, roof, and steel plates on both sides of the vehicle, such as a VIPV. Therefore, considering various vehicle spaces to maximize the power output of future PV-powered EVs is essential.

Table 1. Summary of previous studies on the PV potential assessment of solar mobility.

References	Type	Module Attachment	Slope/Aspect of Pathway	Temporal Unit	Validation
Seo [29]	Solar car	Roof	Not considered	Hourly	No
Oh et al. [30]	Solar bus	Roof	Not considered	Minutely	Yes
Kim et al. [31]	Solar train	Roof	Not considered	Minutely	No
This study	Solar car	Roof, rear window, side doors	Considered	<Minutely	Yes

The aim of this study is to analyze the potential and change patterns of four modules (roof, rear window, left door, and right door) based on the time and driving route of a PV-powered EV. To this end, this study investigates the effects of change on (1) solar irradiation, (2) solar incidence angle for each module, defined by the following three factors:

Sun position, module position (inclination and azimuth), and road section inclination and azimuth and (3) shaded area. Additionally, we discuss the effectiveness of the rear window module or door modules on both sides compared to the roof module. To this end, this study compares the simulated PV potential with the observed values obtained via field experiments.

2. Methodology

2.1. Study Area

Kangwon National University in Samcheok city, Gangwon-do, Korea, was selected as the study area to assess and validate the potential power output based on the driving time and route of the PV-powered EV. This location was selected as the study area because various cases of PV potential can be analyzed based on the variations in inclination and direction of the module while driving. The latitude and longitude of the study area are $37^{\circ}26'$ and $109^{\circ}09'$, respectively, and the total area is approximately $318,000\text{ m}^2$. Considering the safety of pedestrians at the university, the experiment was conducted on roads of 3135 m length.

To indicate that the characteristics of solar PV potential vary depending on tilt, azimuth, and shadow, the pathway is divided into seventeen sections (yellow circles), as shown in Figure 1a. Each section has various inclinations and azimuths, including flat terrain, and the road section numbers indicate the path sequence. In Figure 1a, the point on the right side of road section No. 1 (hereafter, section 1), located in the south, is the main gate of the campus corresponding to the lowest point of the study area. Figure 1b shows the upward slope roads (for reference, we tried to distinguish the term by naming the 'inclination' of module attached to the car as 'slope' of the road section) of the study area in the 3D aerial image. section 1, from the main gate to the center of the university, has an inclination of 12° (degrees), and section 2, connecting the center, has an inclination of 8° . In Figure 1a, the grey area, except for the southern part, corresponds to the campus area. The upper left corner (sections 7–12) is a hilly terrain with the highest elevation, and the right region (sections 3, 4, and 15) is relatively lower. Sections 5 and 6, which are two regions at different elevations, had a slope of 7° (Figure 1b). Considering that the upper direction of the map is north, the azimuth of the driving road is different for each section. Therefore, a detailed description is omitted.

2.2. Settings and Driving Scenarios of PV-Powered EV

To evaluate the potential power output based on the time and driving route of the PV-powered EV, modules were attached to the four exterior surfaces of the vehicle, as shown in Figure 2a. Assuming that the car is heading north, module A is attached to the roof of the car (inclination angle of 0° from the flat ground, no azimuth), module B is attached to the inclined rear window (inclination of 30° , azimuth of 180° from north), module C to the left door (inclination of 90° , azimuth of 270°), and module D (inclination of 90° , azimuth of 90°) to the right door. Figure 2b shows the various factors that affect the amount of power generated by the attached modules, including variation in irradiation with time, variation in solar incidence angles, and types of solar cells. For the details of background theories and equations of solar incidence angles, see the Kim et al. [31]. The inclination and azimuth of the modules attached to the four sides are different and affected by the slope and main direction of the driving road, as shown in Figure 2b.

The study area includes the flat land and various inclined roads with diverse directions. On a sloped road that is not flat, the inclinations of modules A and B and azimuths of modules C and D are different depending on the direction of the driving route. The solar insolation value of the study area varied with the moving time. Therefore, we compared and analyzed the PV potential of the four modules for various cases based on the time and driving route of PV-powered EV.

In this study, it is assumed that the aforementioned vehicle drives at a constant speed of 20 km/h in sections 1 to 17 with various inclinations and azimuths. As the total length

of the road is 3135 m, the total driving time is 564 s, which is less than 10 min; hence, the insolation value is assumed to be constant. Therefore, the PV potential for the four modules of the photovoltaic EV was simulated using individual and total values for each section. Additionally, by assuming that the study area was driven three times at 9:00, 12:00, and 15:00 at different sun positions during the day, the difference in the PV potential based on the moving time of the PV-powered EV was analyzed.

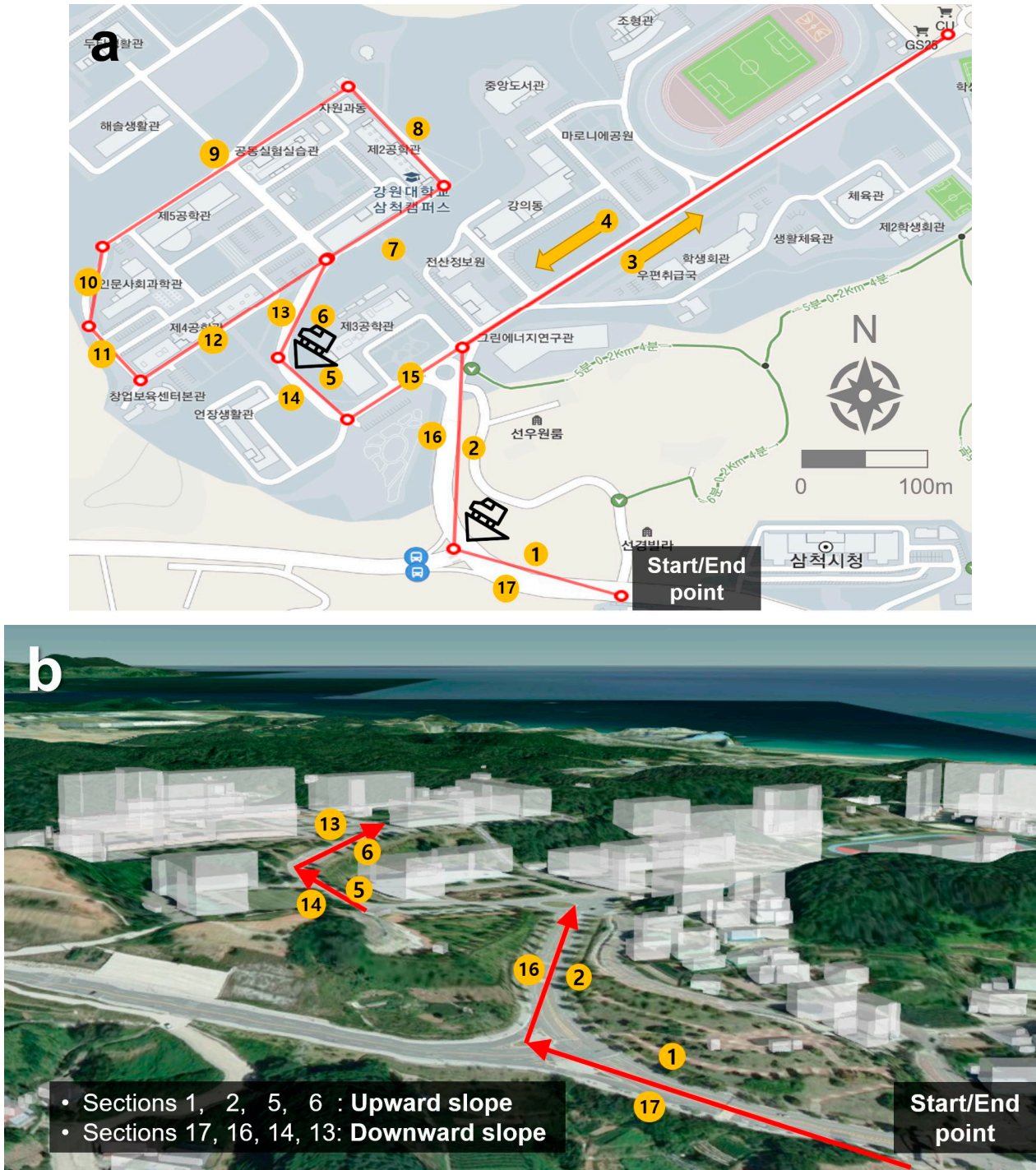


Figure 1. Study area (a) map with 17 driving sections with a different slope and azimuth (Korean labels in the map indicate the building name); (b) 3D aerial view of sloped roads (image sourced from <https://www.vworld.kr/>, accessed on 20 December 2022).

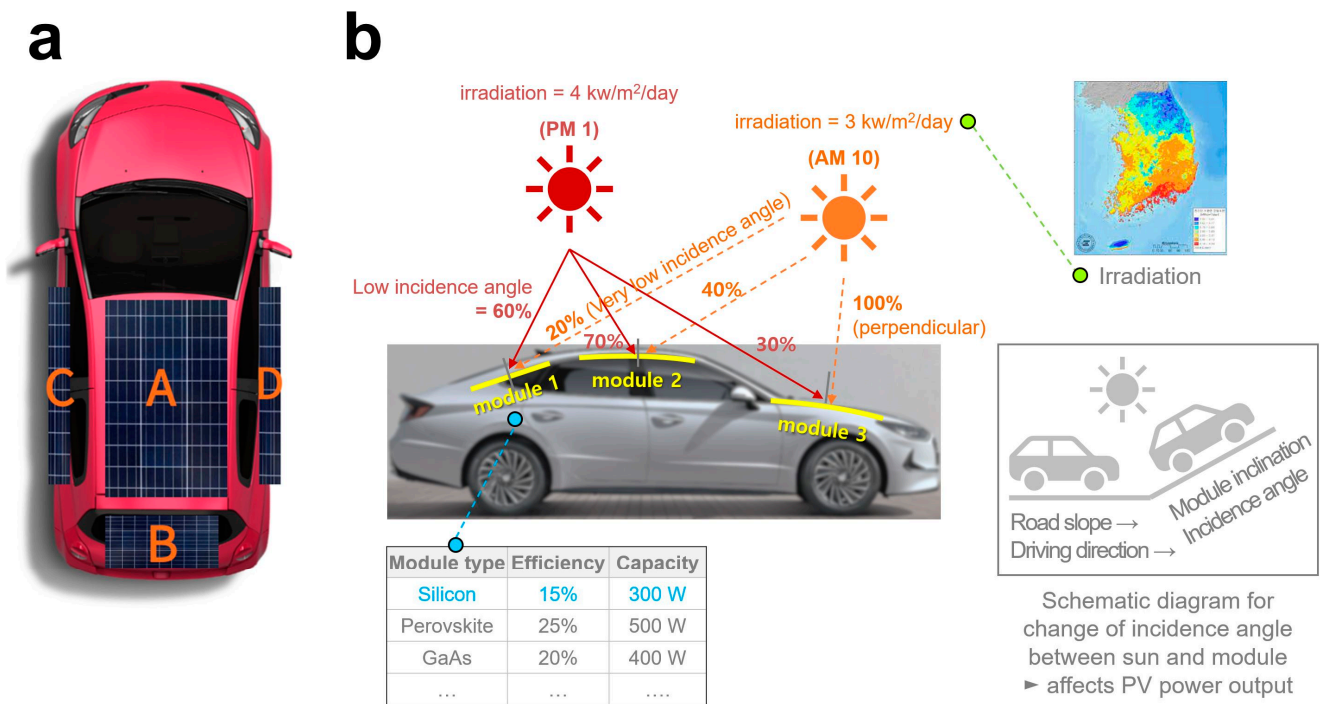


Figure 2. Modules attached to the vehicle (a) position of four modules (A: roof, B: rear window, C: left door, D: right door); (b) factors affecting the PV-powered EV potential.

2.3. Estimation of PV Potential from PV-Powered EV

The research procedure was designed to evaluate the potential power output based on the time and driving route of the PV-powered EV (Figure 3), which mainly consists of the evaluation and verification of the generation potential of PV-powered EV. However, this section only discusses the evaluation. First, considering the meteorological characteristics of the study area, we calculated the specifications and design methods of modules/inverters and the approximate power output potential based on 100% light-receiving efficiency. Second, the actual power output potential was evaluated by modeling the area shaded by the surrounding buildings and topography of the study area and applying it to the driving route.

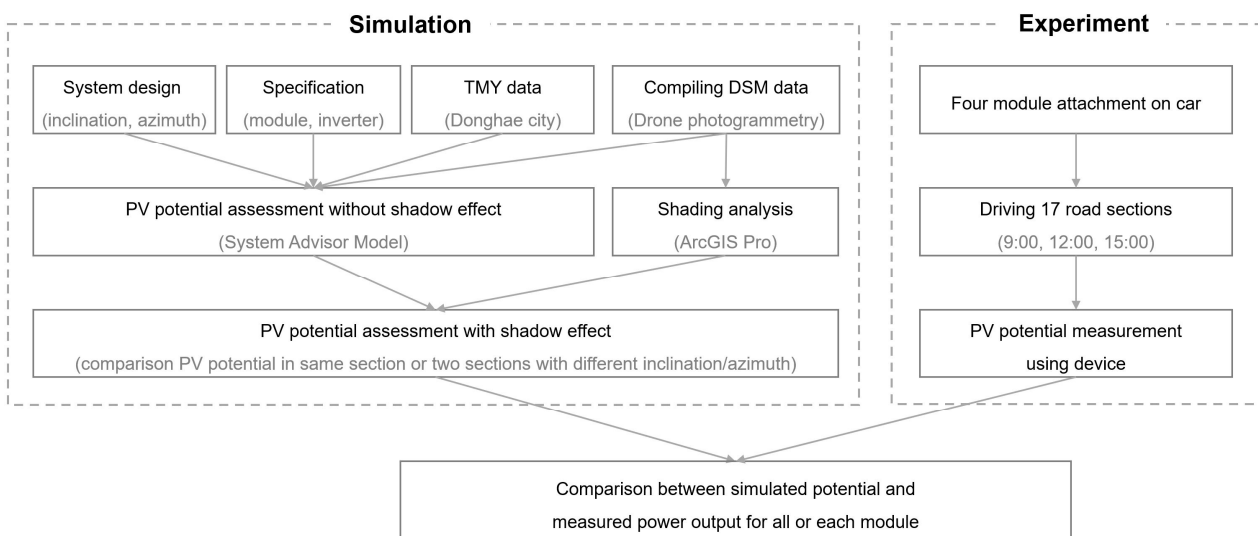


Figure 3. Flowchart for the assessment of PV potential from PV-powered EV.

2.3.1. Estimation of PV Potential Excluding Shadow Effect

To evaluate the PV potential (excluding shaded areas), we used the System Advisor Model (SAM) software developed by the National Renewable Laboratory (NREL), which is a new and renewable energy system. SAM was used as an analysis tool because it has been used in numerous photovoltaic power output projects owing to its accessibility as a free and open-source software that produces reliable and diverse results [32]. SAM requires meteorological characteristics of the desired region, specifications (performance), and design values (type, installation conditions, and other factors) of the module/inverter as input data to evaluate the potential of the photovoltaic power output.

To reflect the meteorological characteristics of the study area, typical meteorological year (TMY) data for the area near the study area were purchased and used on the SolarGIS website. TMY data are the meteorological data collected hourly for a year by selecting a representative year for each month based on the long-term meteorological database, including various meteorological factors such as insolation, dry bulb temperature, and wind speed.

Table 2 lists the model names and physical specifications of the modules attached to the four sides of the vehicle. The smf-175W model was selected for module A with a rated capacity of 175 W, smf-100W model for module B with a rated capacity of 100 W, and fs40W model for modules C and D with a rated capacity of 40 W. For the inverters, the Enphase Energy Inc's IQ7PD-72-2-US model was selected for modules A and B, and Enphase Energy Inc's IQ7PD-84-2-US model was selected for modules C and D. The module was selected considering the area of each part of the vehicle. However, because this study aimed to analyze the differences and variations in the potential solar power output with the module attachment position, the results were presented assuming that all four module capacities were 100 W.

Table 2. Specifications of the PV module and inverter set to PV powered EV.

PV System	Items	Module A	Module B	Module C	Module D
Module	Model	smf-175w	smf-100w	fs40w	fs40w
	Rated maximum power (P_{max})	175 W	100 W	40 W	40 W
	Efficiency	17.30%	15.49%	19.60%	19.60%
Inverter	Attaching position	Roof	Rear window	Left door	Right door
	Efficiency	96%	96%	96%	96%
	Inclination (on flat area)	0°	30°	90°	90°
System design	Azimuth (when car is heading north)	N/A	South	West	East
	Tracking mode	Fixed	Fixed	Fixed	Fixed

The design values of the photovoltaic module include the type, installation inclination, installation azimuth, and the set design values, as listed in Table 2. However, this is based on the original characteristics of the module attached to the vehicle (i.e., when the vehicle is stopped on a flat surface). During actual driving, the slope and azimuth of the module change for each section based on the road characteristics, and the corresponding values are input to the SAM. As module A is flatly attached to the roof, only the inclination varies with the characteristics of the road, whereas in module B, the inclination and azimuth vary. In modules C and D, the azimuth varied; however, the inclination was fixed at 90°.

Thus, the generation potential of a PV-powered EV can be roughly evaluated using the three types of data and SAM software. Owing to the short driving time, we calculated the PV potential for each module in the unit of seconds. The PV potential for each section was evaluated by accumulating the driving time required for each section in seconds. However, this corresponds to the case wherein the shadow effect in the pathway is neglected, i.e., assuming 100% light-receiving efficiency. Therefore, the shaded area should be considered while evaluating the actual photovoltaic power output potential.

2.3.2. Estimation of PV Potential Considering the Shadow Effect

The results derived thus far do not reflect the shadow effect defined by the surrounding environment, such as terrain and buildings. However, shadows have a significant effect on reducing the solar power output. Therefore, we attempted to predict the actual solar power output potential by reflecting the shadow effect of the surrounding topography or buildings in the study area.

The study area was photographed using a DJI Phantom 4 Pro V2.0 drone. Thereafter, Pix4D Mapper Pro software was used to create a 3D digital surface model (DSM) data with a spatial resolution of 0.5 m for the study area. The positions of the sun (altitude and azimuth) at 9:00, 12:00, and 15:00 in December were obtained from the Korea Astronomy Space Science Institute (<http://www.kasi.re.kr/>, accessed on 20 December 2022). By entering the DSM and sun's position data in the hillshade tool (shading modeler) of the ArcGIS Pro software, the hourly shaded areas for the seventeen sections were modeled. The criterion for shaded area analysis was determined to adopt a conservative approach in estimating the potential power output because the ratio of shaded area is highest in December. Finally, the actual power output potential reflected by the shadow effect was evaluated by calculating the shaded-area ratio overlapping with the road.

2.4. Measurement of PV Power Output via Field Experiments

In this study, outdoor experiment was conducted to compare the results of evaluating the PV potential of PV-powered EV obtained from the SAM-based simulation predicted. As shown in Figure 4, modules were attached to the four sides of the vehicle (roof, rear wind shield, left door, and right door), and the experiment was performed at 9:00, 12:00, and 15:00 on a sunny day in December 2022. The power output was measured when the vehicle drove at a constant speed of 20 km/h. Subsequently, we compared and analyzed the difference and change patterns of the PV potential's predicted and experimental values based on the travel time and driving route (17 sections).

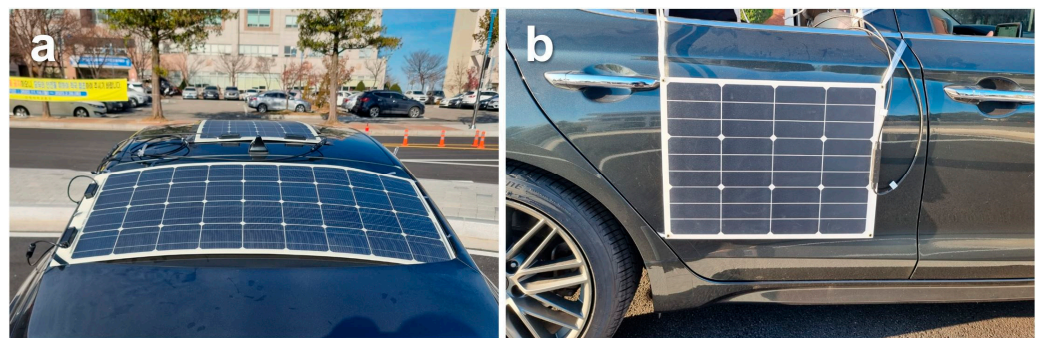


Figure 4. PV modules attached on the car for field experiment. (a) Modules A and B, (b) module D.

3. Results

3.1. PV Potential of the Entire Section

Herein, we present the evaluation results of the potential power output considering the actual length of the road and neglecting the shadow effect, as the PV-powered EV traversed the 17 sections. Figure 5 shows the expected PV potential corresponding to the travel time (9:00, 12:00, and 15:00) when the vehicle was driven in all sections of the study area. The PV potential was maximum at 12:00, when the sun's insolation was maximum, and it gradually decreased for all four modules between 9:00 and 15:00.

Figure 6 shows the individual potential PV power output of the module for all sections. For module A, the generation potential at 12:00 was the maximum because it was attached in parallel to the roof of the vehicle and thus it is not being caused by the azimuth under the sun's highest altitude at 12:00. Contrastingly, for modules C and D, the potential was higher at 9:00 or 15:00 compared 12:00 because the installation inclination of the two modules is 90°, and the angle of incidence is very small when the sun's altitude is maximum.

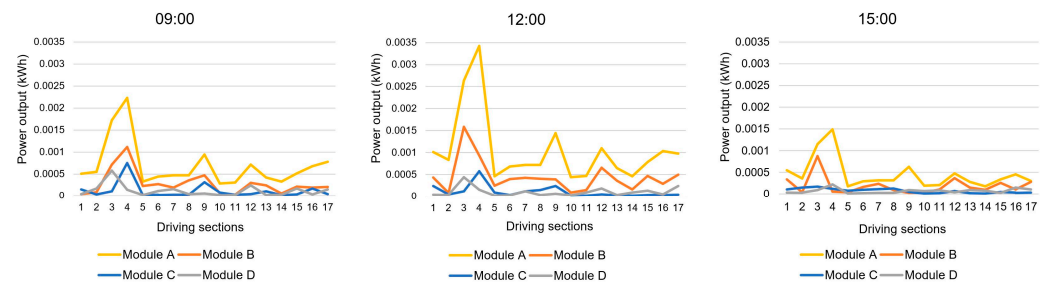


Figure 5. Graphs of PV potential of driving sections over time for all four modules.

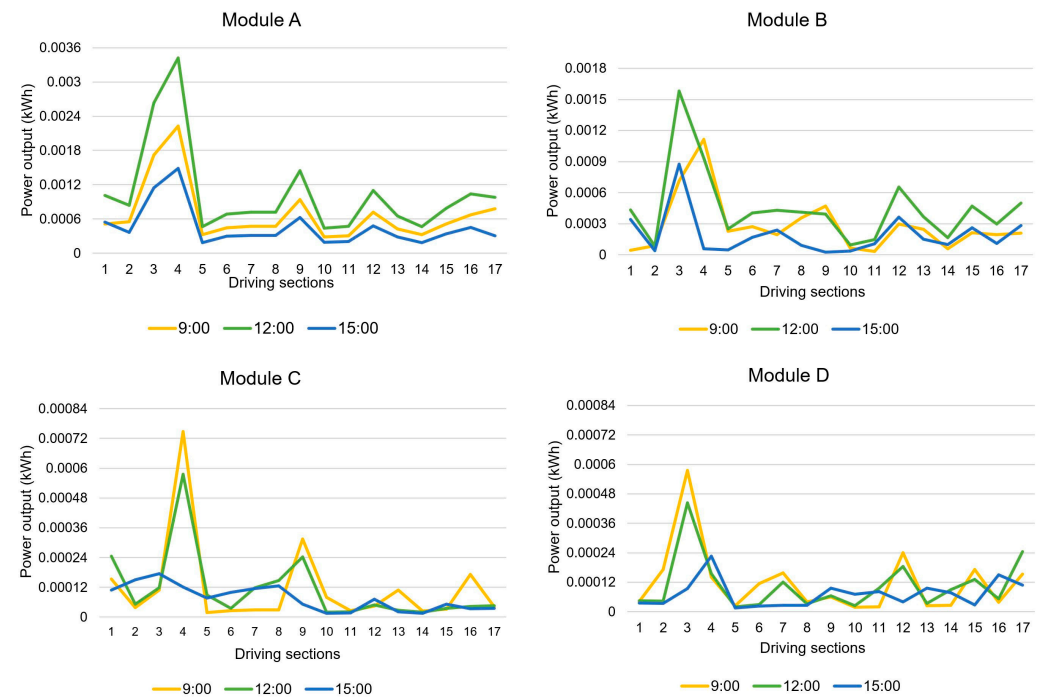


Figure 6. Graphs of the PV potential of the driving sections over time for each module.

Figure 7 shows the change in the solar PV potential of modules C and D over the entire driving range, which is a consequence of assuming the length of all driving sections to be 200 m to effectively express variations in the potential amount contradicting modules C and D. At 9:00 or 15:00, when the angle of incidence of sun is closer to the vertical, the PV potential of the two modules in the majority of sections exhibits a spiral-like form (inverse proportion) because the two modules face opposite directions (azimuths).

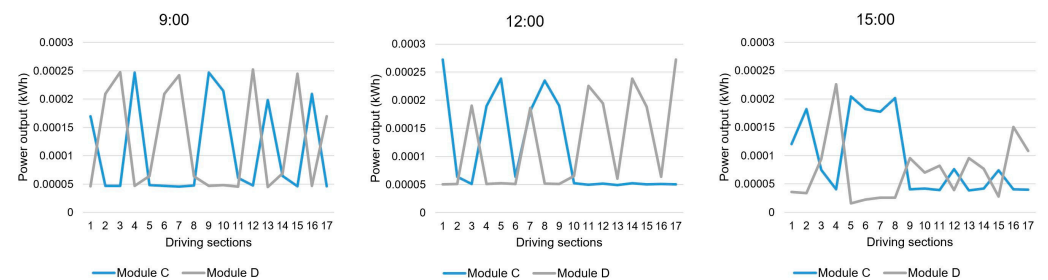


Figure 7. Graphs of the PV potential of the driving sections between modules C and D.

3.2. Comparison of PV Potential in Individual Sections

The solar PV potential is significantly affected by the module capacity and number of sunshine hours. Therefore, to compare and analyze the variation in potential power output owing to the module’s angle of inclination and azimuth with the sun’s position and

driving path, it is crucial to unify the module’s capacity and sunshine time (the length of the driving section). Hence, the capacity of the four modules was set to $100 W_p$, and the lengths of the driving sections (minimum 75 m to maximum 605 m) were unified (assumed) to 200 m. The modules were analyzed based on the characteristics of each section and variations in potential.

3.2.1. Comparison of PV Potential of the Four Modules in Same Section

Figure 8 shows the evaluation results of the PV potential of modules based on the travel time in section 4, which is a flat road. The number in the yellow circle is the section number and the arrow indicates the direction of vehicle motion. The numbers in orange circles indicate the positions of the sun at 9:00, 12:00, and 15:00, which aids in visually understanding the angle of sun incidence to the module attached to the vehicle by showing the position of the sun over time. Considering the hourly position of the sun in the study area, the position of the graph is shown on the right, lower right, and lower left.

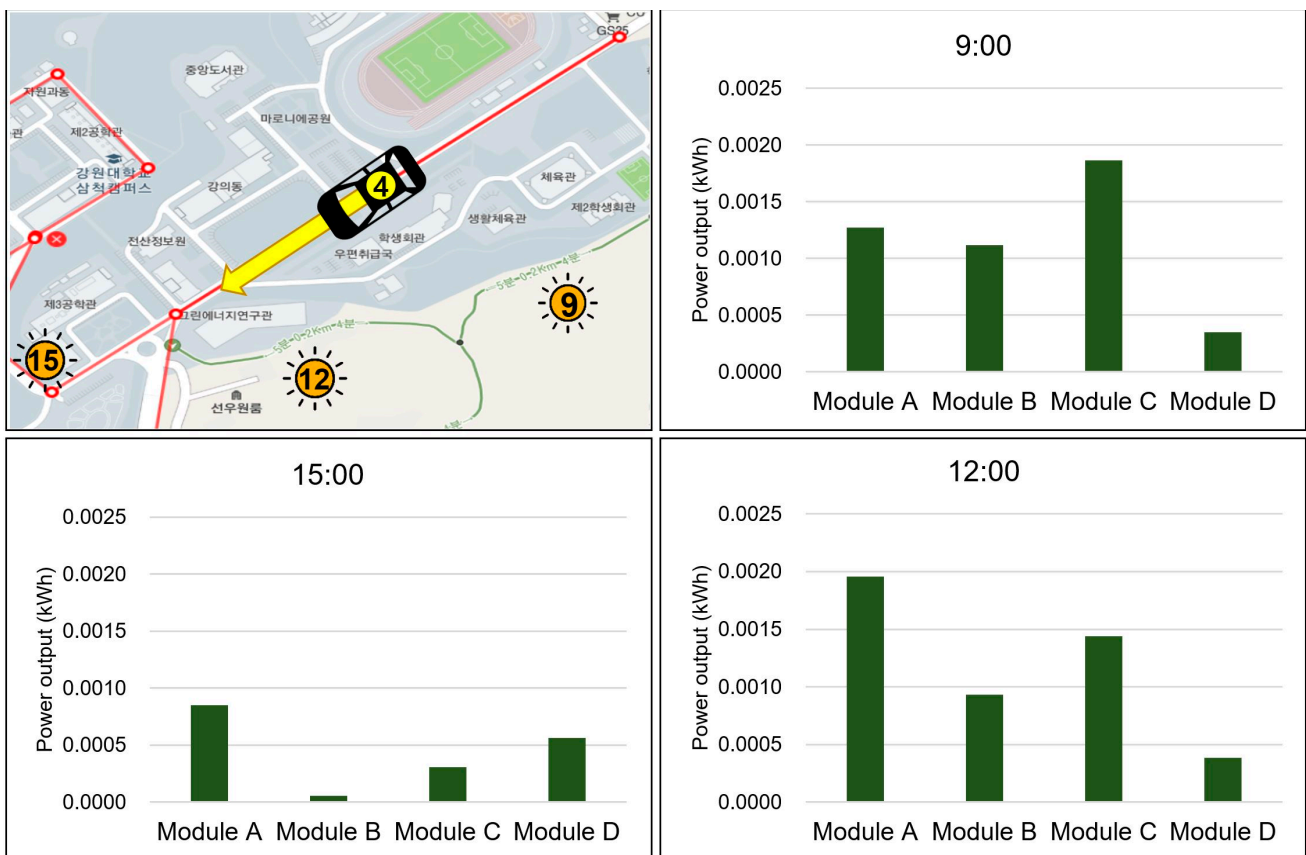


Figure 8. Comparison of PV potentials of four modules at different time in section 4 (Korean labels in the map indicate the building name).

At 9:00, the potential solar power output for each module is in the order C, A, B, and D. Module C, which is attached to the left side of the vehicle, faces southeast toward the sun, and at 9:00 a.m., the sun is at a low altitude; therefore, the sunlight enters the module almost vertically. Therefore, the PV potential of module C was the maximum. The inclination of module A was 0° , and the angle of incidence was small owing to the sun’s low altitude. As module B has an inclination of 30° in the northeast direction, its light receiving efficiency is less than that of module A. As module D faced northwest, opposite to the direction of the sun, its PV potential was the minimum.

Contrastingly, because the sun is located in the southwest direction at 15:00, the PV potentials of the remaining three modules, except module A, which is unaffected by the azimuth, exhibit a large difference. For module B attached to the rear wind shield of

the vehicle, the PV potential was approximately zero because the module’s azimuth and direction of sunlight were the same. Additionally, at 15:00, solar rays are directed to the northeast, whereas module C is directed to the southeast; therefore, its PV potential is considerably lower than that at 9:00.

The altitude and insolation of the sun are highest at 12:00. Therefore, the angle of incidence of the sun on module A is almost vertical, and its PV potential is the maximum. Additionally, the PV potential of the remaining modules were in the order C, B, and D. Herein, the azimuths of each module are southeast, northeast, and northwest. While module C is not in a vertical relationship, the incident angle of sunlight is closer to the vertical; hence, it exhibits the second-highest power potential.

3.2.2. Comparison of PV Potential in Two Sections with Different Azimuth (Same Slope)

The PV potential of each module was compared and analyzed in two sections with the same slope but different azimuths. In the cases of sections 3 and 4, where the driving directions are opposite (180° difference), and sections 7 and 8, where the azimuths differ by 90°, are presented.

Figure 9 shows the modules’ PV potential based on travel time in sections 3 and 4, which were selected as the comparison target sections because both roads are flat and the driving directions are opposite (180° difference). Module A exhibited the same PV potential in both sections because the inclination was 0°; hence, the azimuth was not defined in the two flat sections regardless of the moving time. As the solar radiation varies throughout the day, the PV potential differs depending on the time of movement (in the order 12:00, 9:00, and 15:00). The azimuths of modules C and D in section 3 are northwest and southeast, respectively, and the azimuths of modules C and D in section 4 are southeast and northwest, respectively; hence, the PV potential exhibits an opposite trend. Therefore, the PV potential of module C in section 3 is approximately equal to that of module D in section 4.

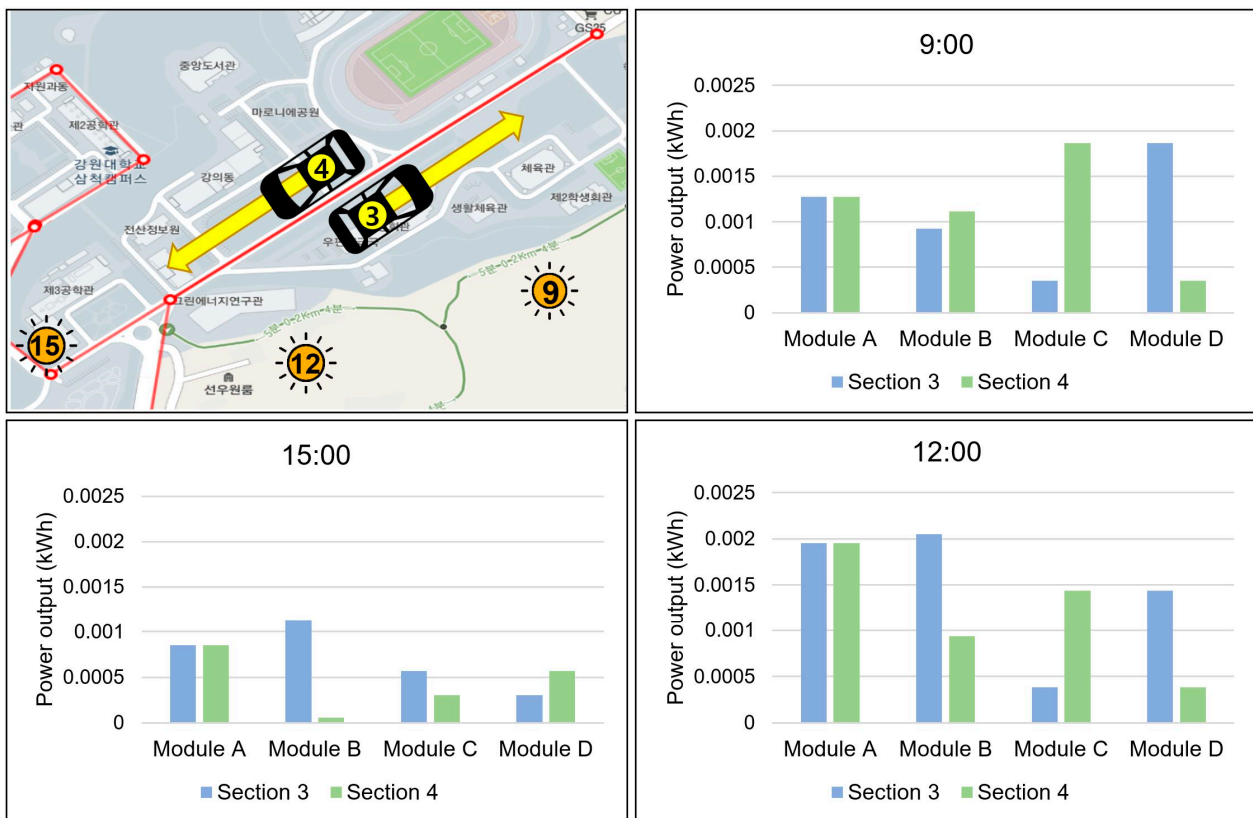


Figure 9. Comparison of PV potentials of four modules by time in section 3 and section 4 in opposite azimuth (Korean labels in the map indicate the building name).

Figure 10 shows the PV potential of the modules based on travel time in sections 7 and 8. The two sections were selected as the comparison target sections because the driving directions were flat and orthogonal. At 12:00, the PV potential and insolation were maximum. At 9:00, the PV potential of module B was higher in section 8 compared to section 7 because in section 8, the module faces southeast toward the sun, whereas it faces southwest in section 7. For module C, the PV potential was low because it did not face the sun in either section at 9:00. For module D, the PV potential was high in section 7 because it faced the direction of the sun. Contrastingly, in section 8, the PV potential was low because it faced northeast. At 12:00, the sun is in the south, and module B faces southwest and southeast in sections 7 and 8, respectively. As the angle of incidence of sunlight with module B in the two sections are almost similar, the PV potential is approximately equal. For module C, the PV potential is small in section 7 because it faces the opposite direction to the sun, whereas in section 8 it faces southwest; hence, the power output potential is relatively high.

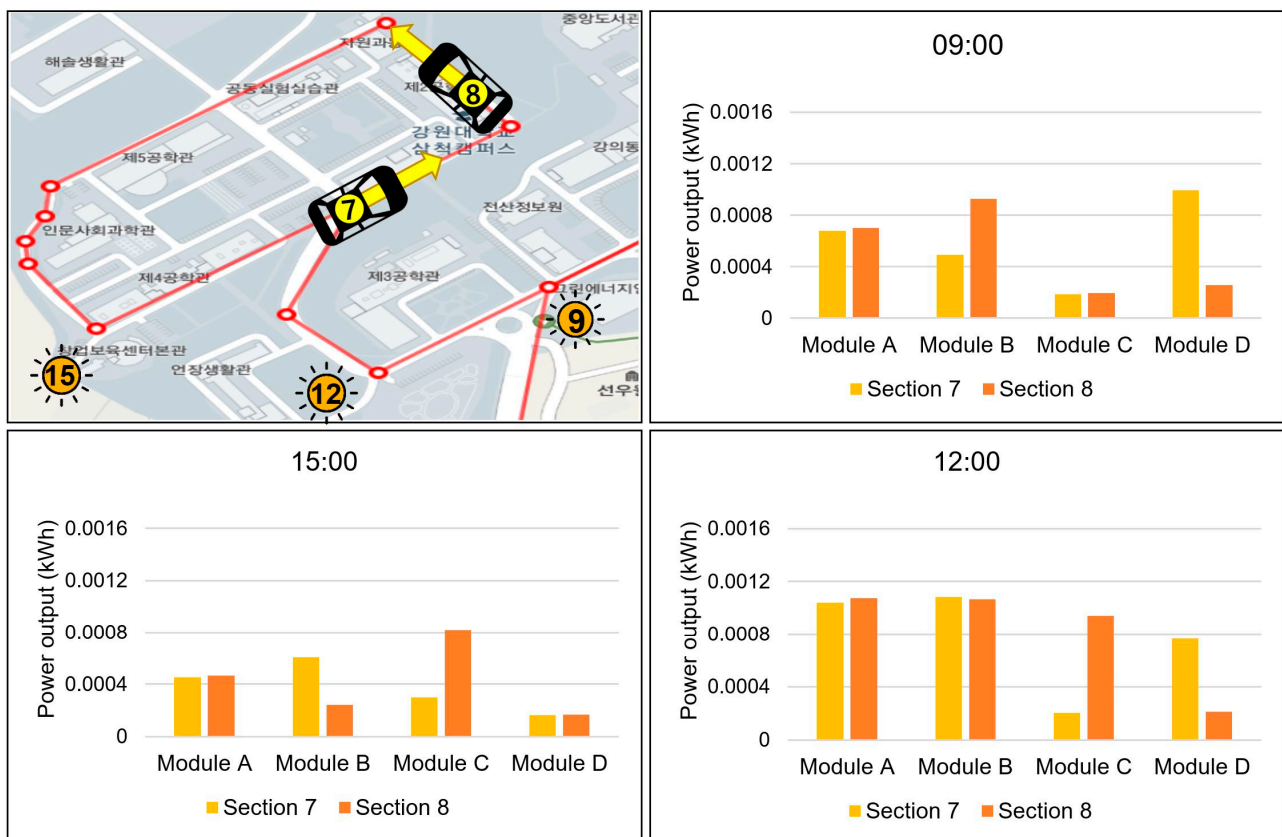


Figure 10. Comparison of PV potential by time between sections 7 and 8 in different azimuth (Korean labels in the map indicate the building name).

The results indicate that the amount of power output expected for each module is significantly different based on the relationship between the position of the sun and vehicle’s moving time, and the azimuth of the module and driving path.

3.2.3. Comparison of PV Potential in Two Sections with Different Slopes (Same Azimuth)

The PV potential of each module was compared and analyzed in two sections regarding the same azimuth and different inclinations. Figure 11 shows the PV potential of the module based on the travel time in sections 10 and 13; the former is a flat road with a slope of 0°, and the latter is a downhill section with a slope of 7°. Variation in the slope angle of the road affected modules A and B. As section 10 is flat, modules A and B maintain their original inclination (0° for module A and 30° for module B). However, in section 13,

module A and B have an angle of -7° and -23° , respectively. Therefore, the PV potential of module B is always greater in section 13 compared to section 10. Contrastingly, modules C and D attached to the left and right sides of the vehicle are hardly affected by the variation in slopes; hence, there is no difference in the PV potential of these two sections.

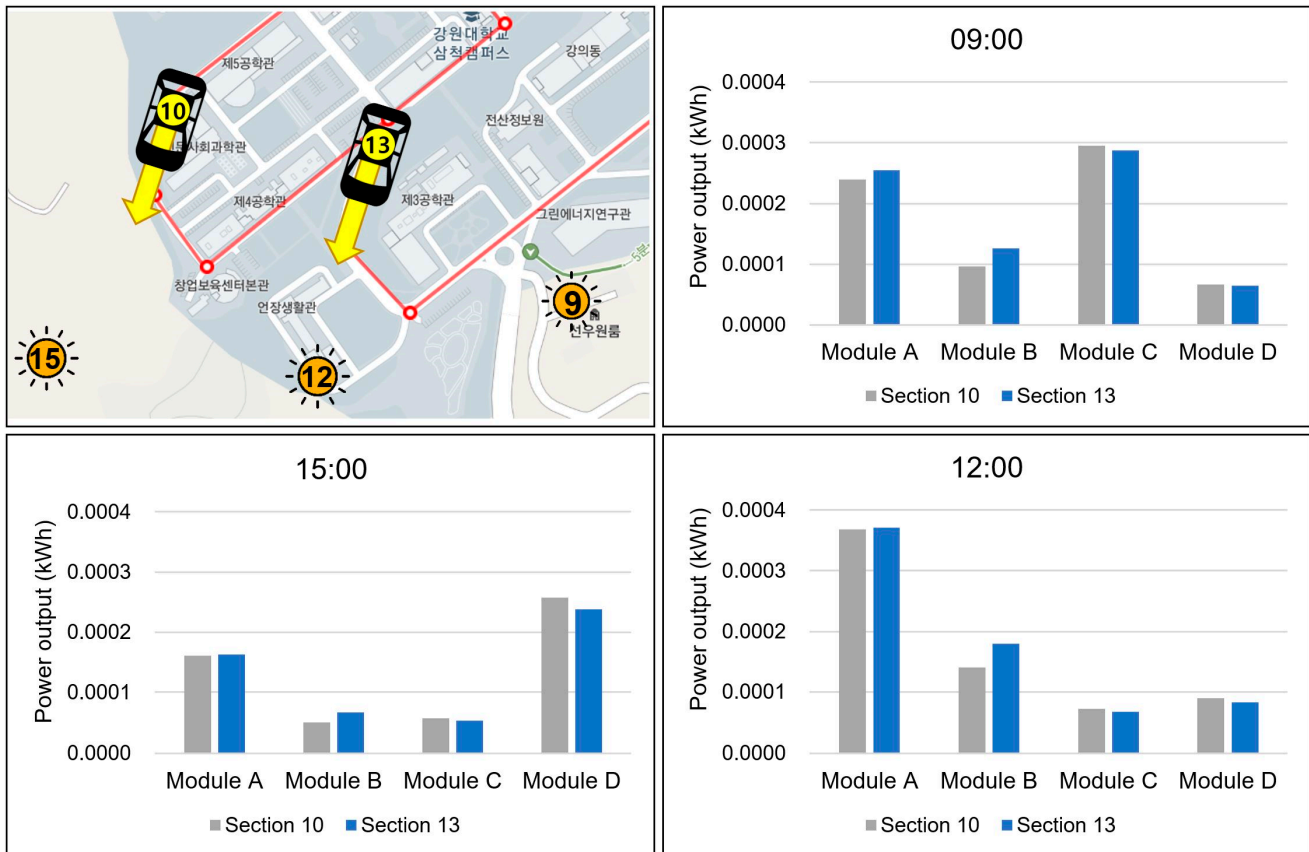


Figure 11. Comparison of PV potential by time between section 10 and section 13 for different slopes (Korean labels in the map indicate the building name).

3.3. Estimation of PV Potential Considering the Shaded Areas

Table 3 shows the ratio of shaded area at 9:00, 12:00, and 15:00 in December for all sections of the study area; the maximum and minimum values were 18.5% and 100%, respectively. Therefore, all driving sections within the study area were affected by shadows. Furthermore, in this study area, the ratio of shaded area by hour was the highest at 9:00 (67.1%), followed by 47.4% (12:00), and 40.9% (15:00).

In the absence of shadow effect, the PV potential of the PV-powered EV is expected to be 0.0365, 0.0439, and 0.0236 kWh at 9:00, 12:00, and 15:00, respectively. In the presence of shadow effect, the expected PV potentials are 0.0117, 0.0225, and 0.0133 kWh at 9:00, 12:00, and 15:00, respectively. Additionally, the average PV potential without the shadow effect is 0.0347 kWh, and the average PV potential with the shadow effect is expected to be 0.0158 kWh. This corresponds to a difference of 0.0189 kWh based on the presence or absence of shadows when driving the entire section once, which is approximately twice the difference. Therefore, shadows have a significant effect on the potential of the solar power output.

3.4. Comparison between Estimated and Measured PV Potentials through Field Experiment

The power output of the car with the attached modules was measured via a field experiment in the study area. The experimental value was compared and analyzed with the predicted value of the PV potential derived previously. However, various uncertainty factors exist in the field, which differ from the conditions assumed in the evaluation.

Therefore, rather than focusing on the comparison between the accuracy of the predicted and experimental values, we attempted to analyze the similarity of their change patterns. In previous studies, there were cases wherein the predicted value of the power output for the module attached to the roof of the mobile was verified; however, only a few cases of the rear wind shield of the PV-powered EV were considered. Therefore, in this study, module B, which is influenced by variations in the slope of the road, was selected as the verification target.

Table 3. Ratio of shaded area and PV potential with/without shadow effect in each section.

Sections	Distance (m)	PV Potential (kWh) (without Shadow)			Shadow (Ratio)			PV Potential (kWh) (with Shadow)		
		9:00	12:00	15:00	9:00	12:00	15:00	9:00	12:00	15:00
1	180	0.0015	0.0029	0.0016	35.0%	25.0%	25.0%	0.0010	0.0022	0.0012
2	165	0.0017	0.0014	0.0013	73.7%	25.0%	25.0%	0.0004	0.0010	0.0010
3	465	0.0059	0.0070	0.0034	88.0%	70.5%	39.6%	0.0007	0.0021	0.0020
4	605	0.0078	0.0080	0.0033	74.4%	37.2%	26.2%	0.0020	0.0050	0.0024
5	75	0.0008	0.0013	0.0007	86.0%	25.0%	84.8%	0.0001	0.0009	0.0001
6	110	0.0014	0.0014	0.0011	41.2%	25.0%	45.6%	0.0008	0.0011	0.0006
7	130	0.0016	0.0023	0.0013	78.4%	66.8%	42.9%	0.0003	0.0008	0.0007
8	125	0.0012	0.0020	0.0012	62.6%	68.8%	93.1%	0.0004	0.0006	0.0001
9	255	0.0033	0.0034	0.0014	87.0%	77.7%	18.5%	0.0004	0.0008	0.0011
10	75	0.0008	0.0008	0.0007	100.0%	30.3%	25.0%	0.0000	0.0005	0.0005
11	85	0.0006	0.0012	0.0008	83.4%	57.1%	73.2%	0.0001	0.0005	0.0002
12	195	0.0024	0.0029	0.0014	56.9%	39.7%	27.4%	0.0011	0.0018	0.0010
13	110	0.0013	0.0013	0.0010	41.2%	25.0%	67.3%	0.0008	0.0010	0.0003
14	75	0.0006	0.0012	0.0007	55.7%	76.8%	91.0%	0.0003	0.0003	0.0001
15	140	0.0017	0.0021	0.0010	66.0%	43.3%	30.3%	0.0006	0.0012	0.0007
16	165	0.0019	0.0018	0.0015	28.6%	25.0%	48.4%	0.0014	0.0014	0.0008
17	180	0.0020	0.0029	0.0013	35.9%	52.6%	68.0%	0.0013	0.0014	0.0004
Total	3135	0.0365	0.0439	0.0236	67.1%	47.4%	40.9%	0.0117	0.0225	0.0133

Figure 12 indicates that the variations in the experimental and predicted values of module B’s power output were similar at 9:00 and 15:00, and different at 12:00. The overall variation in power output was similar. However, the trend at 12:00 is attributed to the influence of the partially shaded areas by trees that were not considered in the field.

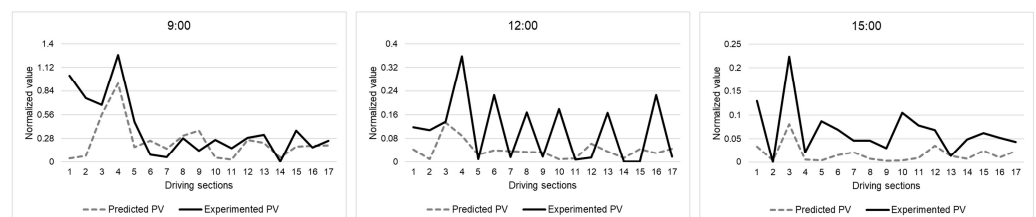


Figure 12. Comparison between normalized PV potentials predicted and observed of module B.

4. Discussion

4.1. Effectiveness of the Modules Attached at the Rear Window and Doors of the Vehicle

Global mobility companies have developed various solar cars or VIPV models. First, the next-generation model uses translucent materials to maintain a sense of openness. Second, it utilizes body-type lightweight solar lids to integrate solar cells into the bonnet, roof, and steel plates on both sides of the vehicle.

In this study, the PV potential of EV was evaluated by attaching modules to the roof, rear window, and side of the vehicle. The potential of module A (roof) was compared to those of modules C and D (both sides). The average PV potential of module A was 0.0125 kWh, and the sum of the PV potentials of modules C and D was 0.0034 kWh. The

potential of the modules C and D was approximately 27% of that of module A because either C or D does not face the sun and produce a low value, or the angle of solar incidence is small. Therefore, the generation potential of the two modules were inversely proportional; hence, the contribution to the increase the vehicle's generation potential was low. Similarly, by comparing the average values of the PV potential of modules A (roof) and B (rear window), the potential power generation of module B was calculated to be approximately 42% of that of module A, which is significantly greater compared to that of the module attached to the side of the vehicle. Therefore, the module attached to the vehicle's rear window of the vehicle contributes significantly to the increase in PV potential.

Of course, in the case of the study area, east-west roads were longer than south-north roads, so this ratio value may change in areas with different road environments. For example, if most of the roads are in the north-south direction, excluding other conditions, the ratio of the potential generation capacity of module B may increase, and the bar rates of modules C and D may decrease. Therefore, the decision to attach the module to the rear window or both sides of the vehicle requires a detailed economic evaluation considering the environmental conditions of the study area.

4.2. Possibility of Expanding Power Output of Future PV-Powered EVs

In this study, the PV potential of a PV-powered EV with silicon solar cells was produced in a short driving time of approximately 10 min. However, the amount of power output that can be expected from potential PV-powered EVs may expand in various aspects owing to the developments in solar cell efficiency, vehicle charging in various cases, diversification of solar mobility, and expansion of production.

First, various types of high-efficiency solar cells have been developed, and the efficiency of the module used in this study is approximately 15%. Recently, the power output efficiency of solar cells has increased, and various types of solar cells, such as transparent and flexible, are being developed. Perovskites, which have a power output efficiency of approximately 30%, can be integrated with PV-powered EVs to double the power output potential. Second, the power output time of PV-powered EV is maximized. Herein, the PV potential was investigated for a vehicle traversing 3135 m of the study area once in 564 s. However, PV potential can be enhanced by increasing the driving time or using 100% of the sunlight time, including non-driving outdoor stops and parking time. Finally, there is a diversification of solar mobility and expansion of production. Herein, only one vehicle was used; however, approximately 24.37 million cars have been registered in Korea. More power output can be expected if the field of mobility utilization combining sunlight into taxis, shuttle buses, and trains, which are driven regularly throughout the year, is diversified and the production is increased.

The PV potential was estimated used the aforementioned conditions (Table 4). Assuming that 243,000 units, or 1% of the vehicles registered in Korea, use PV modules with efficiencies of 15% and 30% and generate power for 6 h a day (9:00 to 15:00) annually, 53,783 GWh and 107,556 GWh of power can be produced. This is a large figure and efforts must be made to expand the supply of PV-powered EV and develop high-efficiency solar cells.

Table 4. Estimation of PV potential from PV-powered EV based on a hypothetical scenario.

Time	PV Potential per Car (kWh)		PV Potential for 243,000 Cars (MWh)	
	Cell Efficiency		Cell Efficiency	
	15%	30%	15%	30%
564 s	0.0158	0.0316	3.84	7.68
1 h	0.1011	0.2022	24.57	49.13
1 day	0.6064	1.2128	147.36	294.71
1 year	221.3298	442.6596	53,783.14	107,556.28

5. Conclusions

In this study, the amount of electricity generated by PV-powered EV on a university campus road was estimated by considering the time and driving route. Unlike previous studies that only considered vehicle roof modules, we evaluated the potential of modules attached to the four sides of the vehicle (roof, rear window, left door, and right door). As a result, the PV potential of module B (rear window) was calculated to be approximately 42% of that of module A (roof). Through the validation experiment, we analyzed the variation in PV potential for each module with the slope and azimuth of the driving section and the time of the day. Additionally, the effectiveness of the module attached to the rear window was compared to that of the roof module. The amount of expected power output for a vehicle running for approximately 10 min was 0.0158 kWh, which is low. In future, the power generation can be significantly increased by improving the cell efficiency and increasing the number of vehicles.

The following should be considered for deriving improved research results. We used TMY data to evaluate the PV potential, which corresponds to the statistical values derived from long-term data. Therefore, it is necessary to take a conservative approach using P90 data to secure the reliability of results in predictions of sub-hours instead of annual or monthly units. Additionally, in the field experiment, the shadows formed by trees did not occur in the modelled shaded area. Herein, DSM could not include some of the trees; however, shadow experimental tools may be used in future. Furthermore, to conceptualize a solar electronic vehicle, an experiment was conducted by attaching a module. However, an experiment using an actual PV-powered EV would be preferable in future.

The results of this study can be used as the base data for designing third-generation solar vehicles. Furthermore, the development of a navigation service for PV-powered EV maximizing the power output and its installation in driverless EV or self-driving taxis may be beneficial for building smart energy cities and developing a sustainable energy industry.

Author Contributions: C.P., H.P., H.J. and J.S. designed, gathered, simulated, and interpreted data; All the authors conducted field experiment; C.P., H.P. and J.S. wrote the paper; J.S. implemented the final work for the paper submission. All authors have read and agreed to the published version of the manuscript.

Funding: This study was supported by (1) Institute of Information & communications Technology Planning & Evaluation (IITP) grant funded by the Korea government (MSIT) (2021-0-01886, Development of UAV-GIS-IoT-AI-M&S convergence digital twin web application for design, evaluation, operation and maintenance of photovoltaic systems) and (2) 2019 Research Grant from Kangwon National University.

Institutional Review Board Statement: Not applicable.

Informed Consent Statement: Not applicable.

Data Availability Statement: Data sharing not applicable.

Conflicts of Interest: The authors declare no conflict of interest.

Abbreviations

The following abbreviations are used in this manuscript. DSM: Digital surface model; EU: European Union; EV: Electric vehicle; HV: Hydrogen vehicle; GHI: Global horizontal irradiance; NREL: National Renewable Energy Laboratory; PV: Photovoltaic; SAM: System Advisor Model; TMY: Typical Meteorological Year; USD: US Dollars; VIPV: Vehicle-integrated photovoltaic.

References

1. Foley, A.; Olabi, A.G. Renewable energy technology developments, trends and policy implications that can underpin the drive for global climate change. *Renew. Sustain. Energy Rev.* **2017**, *68*, 1112–1114. [CrossRef]
2. Koengkan, M.; Fuinhas, J.A.; Teixeira, M.; Kazemzadeh, E.; Auza, A.; Dehdar, F.; Osmani, F. The Capacity of Battery-Electric and Plug-in Hybrid Electric Vehicles to Mitigate CO₂ Emissions: Macroeconomic Evidence from European Union Countries. *World Electr. Veh. J.* **2022**, *13*, 58. [CrossRef]
3. Jakučionytė-Skodienė, M.; Krikštolaitis, R.; Liobikienė, G. The contribution of changes in climate-friendly behaviour, climate change concern and personal responsibility to household greenhouse gas emissions: Heating/cooling and transport activities in the European Union. *Energy* **2022**, *246*, 123387. [CrossRef]
4. Sierra, A.; Reinders, A. Designing innovative solutions for solar-powered electric mobility applications. *Prog. Photovolt. Res. Appl.* **2021**, *29*, 802–818. [CrossRef]
5. Hannan, M.A.; Hoque, M.M.; Mohamed, A.; Ayob, A. Review of energy storage systems for electric vehicle applications: Issues and challenges. *Renew. Sustain. Energy Rev.* **2017**, *69*, 771–789. [CrossRef]
6. Sierra Rodriguez, A.; de Santana, T.; MacGill, I.; Ekins-Daukes, N.J.; Reinders, A. A feasibility study of solar PV-powered electric cars using an interdisciplinary modeling approach for the electricity balance, CO₂ emissions, and economic aspects: The cases of The Netherlands, Norway, Brazil, and Australia. *Prog. Photovolt. Res. Appl.* **2020**, *28*, 517–532. [CrossRef]
7. Yamaguchi, M.; Masuda, T.; Nakado, T.; Zushi, Y.; Araki, K.; Takamoto, T.; Okumura, K.; Satou, A.; Yamada, K.; Ota, Y.; et al. Importance of Developing Photovoltaics-Powered Vehicles. *Energy Power Eng.* **2021**, *13*, 147–162. [CrossRef]
8. Allied Market Research. Available online: <https://www.openpr.com/news/2035028/solar-car-market-growth-to-hit-4-087-6-million-by-2030-solar> (accessed on 15 December 2022).
9. Un-Noor, F.; Padmanaban, S.; Mihet-Popa, L.; Mollah, M.N.; Hossain, E. A comprehensive study of key electric vehicle (EV) components, technologies, challenges, impacts, and future direction of development. *Energies* **2017**, *10*, 1217. [CrossRef]
10. Yamaguchi, M.; Masuda, T.; Araki, K.; Sato, D.; Lee, K.-H.; Kojima, N.; Takamoto, T.; Okumura, K.; Satou, A.; Yamada, K.; et al. Role of PV-Powered Vehicles in Low-Carbon Society and Some Approaches of High-Efficiency Solar Cell Modules for Cars. *Energy Power Eng.* **2020**, *12*, 375–395. [CrossRef]
11. Yamaguchi, M.; Masuda, T.; Araki, K.; Sato, D.; Lee, K.H.; Kojima, N.; Takamoto, T.; Okumura, K.; Satou, A.; Yamada, K.; et al. Development of high-efficiency and low-cost solar cells for PV-powered vehicles application. *Prog. Photovolt. Res. Appl.* **2021**, *29*, 684–693. [CrossRef]
12. Yamaguchi, M.; Ozaki, R.; Nakamura, K.; Lee, K.H.; Kojima, N.; Ohshita, Y.; Masuda, T.; Okumura, K.; Satou, A.; Nakado, T.; et al. Development of High-Efficiency Solar Cell Modules for Photovoltaic-Powered Vehicles. *Sol. RRL* **2021**, *6*, 2100429. [CrossRef]
13. Ye, B.; Jiang, J.; Miao, L.; Yang, P.; Li, J.; Shen, B. Feasibility study of a solar-powered electric vehicle charging station model. *Energies* **2015**, *8*, 13265–13283. [CrossRef]
14. Esfandyari, A.; Norton, B.; Conlon, M.; McCormack, S.J. Performance of a campus photovoltaic electric vehicle charging station in a temperate climate. *Sol. Energy* **2019**, *177*, 762–771. [CrossRef]
15. Goli, P.; Shireen, W. PV powered smart charging station for PHEVs. *Renew. Energy* **2014**, *66*, 280–287. [CrossRef]
16. Cheikh-Mohamad, S.; Sechilariu, M.; Locment, F.; Krim, Y. Pv-powered electric vehicle charging stations: Preliminary requirements and feasibility conditions. *Appl. Sci.* **2021**, *11*, 1770. [CrossRef]
17. Minh, P.V.; Le Quang, S.; Pham, M.H. Technical economic analysis of photovoltaic-powered electric vehicle charging stations under different solar irradiation conditions in Vietnam. *Sustainability* **2021**, *13*, 3528. [CrossRef]
18. Mitova, S.; Henao, A.; Kahsar, R.; Farmer, C.J. Smart Charging for Electric Ride-Hailing Vehicles using Renewables: A San Francisco Case Study. *Int. J. Sustain. Energy Environ. Res.* **2022**, *11*, 67–85. [CrossRef]
19. Deshmukh, S.S.; Pearce, J.M. Electric vehicle charging potential from retail parking lot solar photovoltaic awnings. *Renew. Energy* **2021**, *169*, 608–617. [CrossRef]
20. Farahmand, M.Z.; Javadi, S.; Sadati, S.M.B.; Laaksonen, H.; Shafie-khah, M. Optimal Operation of Solar Powered Electric Vehicle Parking Lots Considering Different Photovoltaic Technologies. *Clean Technol.* **2021**, *3*, 503–518. [CrossRef]
21. Choi, Y.; Kang, B.; Kang, M.; Kim, M.; Lee, S.; Han, S.; Ha, W.; Lee, S.W.; Ahn, S. Analysis of Optimal Location for Campus Solar-powered Electric Vehicle Parking Lots Using a Fisheye Lens Camera. *J. Korean Soc. Miner. Energy Resour. Eng.* **2021**, *58*, 307–318. [CrossRef]
22. Baek, J.; Choi, Y. An Experimental Study on Performance Evaluation of Shading Matrix to Select Optimal Parking Space for Solar-Powered Electric Vehicles. *Sustainability* **2022**, *14*, 14922. [CrossRef]
23. Baek, J.; Choi, Y. Comparative Study on Shading Database Construction for Urban Roads Using 3D Models and Fisheye Images for Efficient Operation of Solar-Powered Electric Vehicles. *Energies* **2022**, *15*, 8228. [CrossRef]
24. Hasicic, M.; Siljak, H. Putting the SC in SCORE: Solar Car Optimized Route Estimation and Smart Cities. In *Modeling and Optimization in Green Logistics*; Springer: Cham, Switzerland, 2020; pp. 75–86. [CrossRef]
25. ur Rehman, N.; Hijazi, M.; Uzair, M. Solar potential assessment of public bus routes for solar buses. *Renew. Energy* **2020**, *156*, 193–200. [CrossRef]
26. Jiang, L.; Hua, Y.; Ma, C.; Liu, X. SunChase: Energy-Efficient Route Planning for Solar-Powered EVs. In Proceedings of the 2017 IEEE 37th International Conference on Distributed Computing Systems (ICDCS), Atlanta, GA, USA, 5–8 June 2017; pp. 383–393. [CrossRef]

27. Artmeier, A.; Haselmayr, J. The Optimal Routing Problem in the Context of Battery-Powered Electric Vehicles. 2020, pp. 1–13. Available online: <https://mediatum.ub.tum.de/993198> (accessed on 20 December 2022).
28. Goli, A.; Golmohammadi, A.-M.; Verdegay, J.-L. Two-echelon electric vehicle routing problem with a developed moth-flame meta-heuristic algorithm. *Oper. Manag. Res.* **2022**, *15*, 891–912. [[CrossRef](#)]
29. Seo, H. Estimation of PV-Powered Electric Vehicle Potential by Hour in the Expressway Using GIS. Master's Thesis, Kangwon National University, Chuncheon, Republic of Korea, 2022.
30. Oh, M.; Kim, S.M.; Park, H.D. Estimation of photovoltaic potential of solar bus in an urban area: Case study in Gwanak, Seoul, Korea. *Renew. Energy* **2020**, *160*, 1335–1348. [[CrossRef](#)]
31. Kim, H.; Ku, J.; Kim, S.M.; Park, H.D. A new GIS-based algorithm to estimate photovoltaic potential of solar train: Case study in Gyeongbu line, Korea. *Renew. Energy* **2022**, *190*, 713–729. [[CrossRef](#)]
32. Suh, J.; Jang, Y.; Choi, Y. Comparison of electric power output observed and estimated from floating photovoltaic systems: A case study on the hapcheon dam, Korea. *Sustainability* **2020**, *12*, 276. [[CrossRef](#)]

Disclaimer/Publisher's Note: The statements, opinions and data contained in all publications are solely those of the individual author(s) and contributor(s) and not of MDPI and/or the editor(s). MDPI and/or the editor(s) disclaim responsibility for any injury to people or property resulting from any ideas, methods, instructions or products referred to in the content.